Molecular Cell, Vol. 12, 75–86, July, 2003, Copyright ©2003 by Cell Press

Structural Basis of Degradation Signal Recognition by SspB, a Specificity-Enhancing Factor for the ClpXP Proteolytic Machine

Hyun Kyu Song[1,2] and Michael J. Eck[1,2,*]
[1]Department of Cancer Biology
Dana-Farber Cancer Institute
44 Binney Street
Boston, Massachusetts 02115
[2]Department of Biological Chemistry
and Molecular Pharmacology
Harvard Medical School
Boston, Massachusetts 02115

Summary

In prokaryotes, incomplete or misfolded polypeptides emanating from a stalled ribosome are marked for degradation by the addition of an 11 residue peptide (AANDENYALAA) to their C terminus. Substrates containing this conserved degradation signal, the SsrA tag, are targeted to specific proteases including ClpXP and ClpAP. SspB was originally characterized as a stringent starvation protein and has been found to bind specifically to SsrA-tagged proteins and to enhance recognition of these proteins by the ClpXP degradation machine. Here, we report the crystal structures of SspB alone and in complex with an SsrA peptide. Unexpectedly, SspB exhibits a fold found in Sm-family RNA binding proteins. The dimeric SspB structures explain the key determinants for recognition of the SsrA tag and define a hydrophobic channel that may bind unfolded substrates.

Introduction

Intracellular protein degradation is a highly regulated process; the proteolytic machinery must select the right substrate in the right place at the right time. In both prokaryotes and eukaryotes, degradation tags are used to mark proteins for degradation. These tags target the marked protein to specific proteases, and regulation is affected by a variety of proteins that modulate both the tagging of substrates and the recognition and degradation of tagged substrates. In eukaryotes, one such targeting mechanism is covalent attachment of ubiquitin chains, which marks proteins for destruction by the 26S proteosome (Hershko and Ciechanover, 1998; Laney and Hochstrasser, 1999; Voges et al., 1999). Ubiquitin-dependent degradation regulates diverse cellular processes, including cell cycle progression, growth factor signal transduction, and transcriptional regulation (Hershko and Ciechanover, 1998; Verma and Deshaies, 2000; Conaway et al., 2002). In eubacteria, one well-characterized tag is an 11 residue polypeptide known as SsrA, which specifically directs marked substrates to the ATP-dependent proteases ClpXP or ClpAP. The SsrA tag is attached *trans*-translationally to the C terminus of nascent polypeptides on stalled ribosomes (Keiler et al., 1996; Withey and Friedman, 2002). The SsrA tag is encoded and coupled to substrates by a unique RNA molecule that combines the activities of both transfer RNA and messenger RNA (tmRNA, also known as 10Sa RNA or SsrA RNA) (Retallack and Friedman, 1995; Keiler et al., 1996). When protein synthesis on the ribosome stalls for any of a variety of reasons (Keiler et al., 1996; Roche and Sauer, 1999; Gillet and Felden, 2001; Roche and Sauer, 2001; Hayes et al., 2002a, 2002b), this quality control mechanism SsrA tags the incomplete nascent protein, thereby promoting its degradation by proteases including ClpXP or ClpAP (Gottesman et al., 1998).

ClpXP and ClpAP are multisubunit protein complexes that promote ATP-dependent degradation of many cellular proteins. ClpXP and ClpAP share a common protease, ClpP, which has a small entrance to an inner proteolytic chamber formed by a double-ring of heptameric subunits (Kessel et al., 1995; Wang et al., 1997). Before degradation, substrates must be bound, unfolded, and translocated into the proteolytic chamber by ClpX or ClpA, which are hexameric AAA+ ATPases belonging to the Clp/Hsp100 family (Gottesman et al., 1997). ClpX and ClpA both recognize SsrA-tagged proteins, but they have distinct preferences for natural substrates (Wojtkowiak et al., 1993; Levchenko et al., 1995; Schweder et al., 1996; Wang et al., 1999). General rules governing substrate recognition have not been elucidated, but it is known that ClpAP, but not ClpXP, can degrade denatured proteins lacking a tag (Hoskins et al., 2000).

The proteolytic specificity of ClpXP and ClpAP can be further regulated by protein factors that modulate recognition of degradation signals by the protease. In *Escherichia coli*, stringent starvation protein B (SspB) (Williams et al., 1994) binds specifically to SsrA-tagged substrates and enhances the recognition of these proteins by ClpX (Levchenko et al., 2000). ClpX and ClpA have recently been shown to interact with different binding determinants in the SsrA tag. Moreover, SspB has been shown to interact with a site that partially overlaps that bound by ClpA, resulting in inhibition of ClpAP-mediated degradation (Flynn et al., 2001). Thus, SspB promotes degradation of SsrA-tagged substrates by ClpXP but inhibits degradation by ClpAP. ClpS, a substrate modulator of the ClpAP machine, inhibits degradation of SsrA-tagged proteins and also triggers release of the prebound SsrA-tagged substrates by interaction with the N-terminal domain of ClpA (Dougan et al., 2002b). The crystal structure of ClpS in complex with the N-terminal domain of ClpA was recently determined (Guo et al., 2002a; Zeth et al., 2002), but no structural information is available for SspB or for the SsrA tag in complex with any binding partner.

In order to better understand recognition of the SsrA tag and the mechanism of delivery SsrA-tagged substrates to ATP-dependant proteases, we have determined the crystal structure of *E. coli* SspB in complex with the SsrA tag. SspB is a central mediator in SsrA-dependent proteolysis and an interesting target for structural studies, as it interacts with at least three different partners including ClpX, an SsrA-tagged substrate, and the ribosome (Levchenko et al., 2000). We report

*Correspondence: eck@red.dfci.harvard.edu

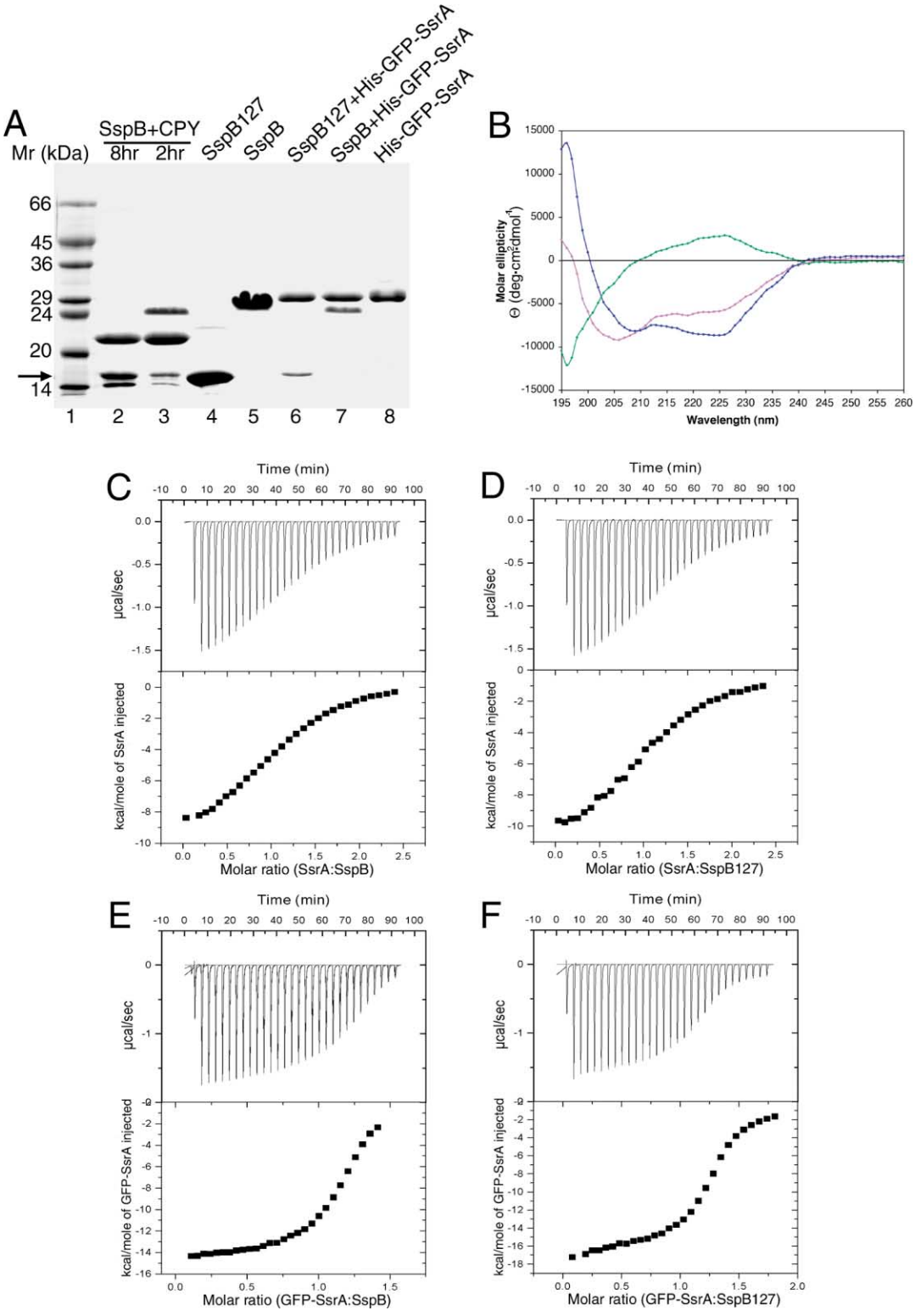

Figure 1. Biochemical Analysis of Purified SspB Proteins

(A) Coomassie stained, SDS-PAGE gel showing limited proteolysis of SspB with carboxypeptidase Y and in vitro binding affinity of full-length and truncated SspB to SsrA-tagged GFP. Purified full-length SspB (lane 5) was treated with carboxypeptidase Y (CPY) for 2 hr (lane 3) or 8 hr (lane 2). The fragment with lower molecular weight (indicated by the arrow) was recloned, expressed, and purified (SspB127, lane 4). His-GFP-SsrA (immobilized on nickel-affinity resin) binds roughly stoichiometric amounts of both wild-type SspB (lane 7) and SspB127 (lane 6).
(B) A difference circular dichroism spectrum (green) was generated by substracting the spectrum of SspB127 (blue) from that of SspB (magenta). The difference spectrum is typical of a random coil, indicating that the residues 128–165 of SspB are mostly unstructured in solution.

here its structure alone and in complex with SsrA at 2.2 and 2.9 Å resolution, respectively. The structure reveals an RNA binding fold termed the "Sm-fold" (Kambach et al., 1999) despite a lack of recognizable sequence similarity with other Sm-fold proteins. The SspB/SsrA complex explains key determinants for recognition of the SsrA peptide and sheds light on recruitment of target proteins to the prokaryotic degradation machine.

Results and Discussion

Biochemical Analysis

Because crystallization of full-length SspB did not initially yield crystals suitable for structure determination, we dissected the SspB molecule using limited proteolysis. Treatment with carboxypeptidase Y yielded a relatively stable fragment containing residues 1–127 of SspB (Figure 1A). This fragment, referred to here as SspB127, was expressed in soluble form in *E. coli* (see Experimental Procedures). Comparison of the circular dichroism spectra of full-length SspB and SspB127 suggests that C-terminal tail (128–165) of SspB is unstructured in the purified protein (Figure 1B). This result is not unexpected, given its proteolytic susceptibility, lack of predicted secondary structure, and amino acid content (3 glycines and 7 prolines in 38 residues; 26.3%) (Figure 2A). In the course of purification we observed that full-length SspB forms stable dimers in solution as recently reported (Wah et al., 2002). Comparison of the gel-filtration profiles of full-length and truncated SspB indicated that SspB127 also forms dimers; thus, the C-terminal tail is not required for dimerization.

We next asked whether removal of the C-terminal tail affected recognition of the SsrA peptide or of an SsrA-tagged substrate (green fluorescent protein, His-GFP-SsrA). His-GFP-SsrA, immobilized on metal-affinity beads, bound approximately stoichiometric amounts of both SspB and SspB127 (Figure 1A, lanes 6 and 7). Furthermore, SspB and SspB127 bind the SsrA tag with essentially identical affinity. Using isothermal titration calorimetry (ITC), we measured dissociation constants (K_D) of 6.16 and 6.21 μM for binding of SspB and SspB127, respectively, to the isolated SsrA peptide (Figures 1C and 1D). SspB binds SsrA-tagged GFP approximately one order of magnitude more tightly than the isolated SsrA tag (Wah et al., 2002); this property is also preserved in the SspB127 (Figures 1E and 1F).

Although the C-terminal tail of SspB does not participate in dimerization or SsrA recognition, it does appear to participate in recognition and activation of the ClpX ATPase. As expected (Wah et al., 2002), we observed approximately 2-fold activation of ClpX upon addition of stoichiometric concentrations of SspB (a stoichiometry of 1 SspB dimer to 1 ClpX hexamer, Figure 2B). However, SspB127 increased ClpX activity only very modestly, even at 4-fold higher concentrations (Figure 2C). These results suggest that the C-terminal tail may become at least partially structured upon binding to ClpX and contribute to allosteric activation of the ATPase.

Crystallization trials with the truncated SspB protein readily yielded tetragonal crystals that diffracted X-rays to 2.2 Å resolution. Cocrystallization of SspB127 with the SsrA tag produced only very poorly ordered crystals, but we did obtain SsrA cocrystals suitable for structure determination using the full-length SspB protein. The SspB127 structure was phased by multiple wavelength anomalous dispersion methods using selenomethionine-substituted protein (see Table 1 and Experimental Procedures). The free SspB127 structure was used as a model for determination of the SspB/SsrA structure by molecular replacement (see Table 1 and Experimental Procedures).

Overall Structure

The SspB homodimer has an elongated shape with approximate dimensions of 70 $\times$ 45 $\times$ 33 Å (Figure 3A). Each monomer is a compact domain (approximately 35 $\times$ 40 $\times$ 32 Å) consisting of a β sandwich capped at one end by a long α helix (Figure 3B). Additional elements of secondary structure include two 3_{10} helices, one in the loop connecting β strands 1 and 2 and the other near the C terminus. The first 4 (Met1-Ser4) and last 16 residues (Glu112-Glu127) of SspB127 are not observed in the electron density and are likely unstructured; the refined model includes residues 5–111 of SspB (Table 1). The structured region of full-length SspB in complex with the SsrA tag is similar (residues 4–111). SDS-PAGE analysis of SspB/SsrA crystals revealed no evidence of proteolytic cleavage; thus, the lack of electron density for the C-terminal residues is likely due to disorder (data not shown).

In spite of a lack of recognizable sequence similarity, the fold of SspB is topologically similar to that of the RNA binding domain of small nuclear ribonucleoproteins (Sm-fold) (Kambach et al., 1999) and more distantly similar to a portion of the ribosome-associated protein L1 (Nevskaya et al., 2000). The structures of SspB, Sm D2, and ribosomal protein L1 are shown in a similar orientation in Figure 4. Superposition of structurally equivalent residues in SspB and Sm D2 protein (PDB ID 1B34, B chain) yields an rms deviation of 3.3 Å for 58 matching Cα atoms, and that of SspB and L1 protein (PDB ID 1CJS) yields an rms deviation of 3.4 Å for 64 matching Cα atoms. Both Sm D2 and L1 bind RNA but in structurally distinct sites. Thus, it is unclear whether the observed structural similarity reflects an evolutionary relationship. Nevertheless, it is interesting to note that SspB protein has been observed to copurify with ribosomes and that GFP-SsrA degradation by ClpXP is increased in the ribosomal fraction (Levchenko et al., 2000). The structural similarity with Sm-fold proteins suggests the possibility that SspB could recognize an RNA component of the ribosome. SsrA-tagged proteins emanating from stalled ribosomes are most likely misfolded and/or unfolded

(C and D) Isothermal titration calorimetric studies of SsrA peptide binding to SspB (C) and SspB127 (D) reveal dissociation constants of 6.16 and 6.22 μM, respectively.

(E and F) Isothermal titration calorimetric studies of His-GFP-SsrA protein binding to SspB (E) and SspB127 (F) reveal dissociation constants of 728 and 695 nM, respectively. The raw heat-release curve in the upper panel is corrected for dilution and integrated in the lower panel (C–F).

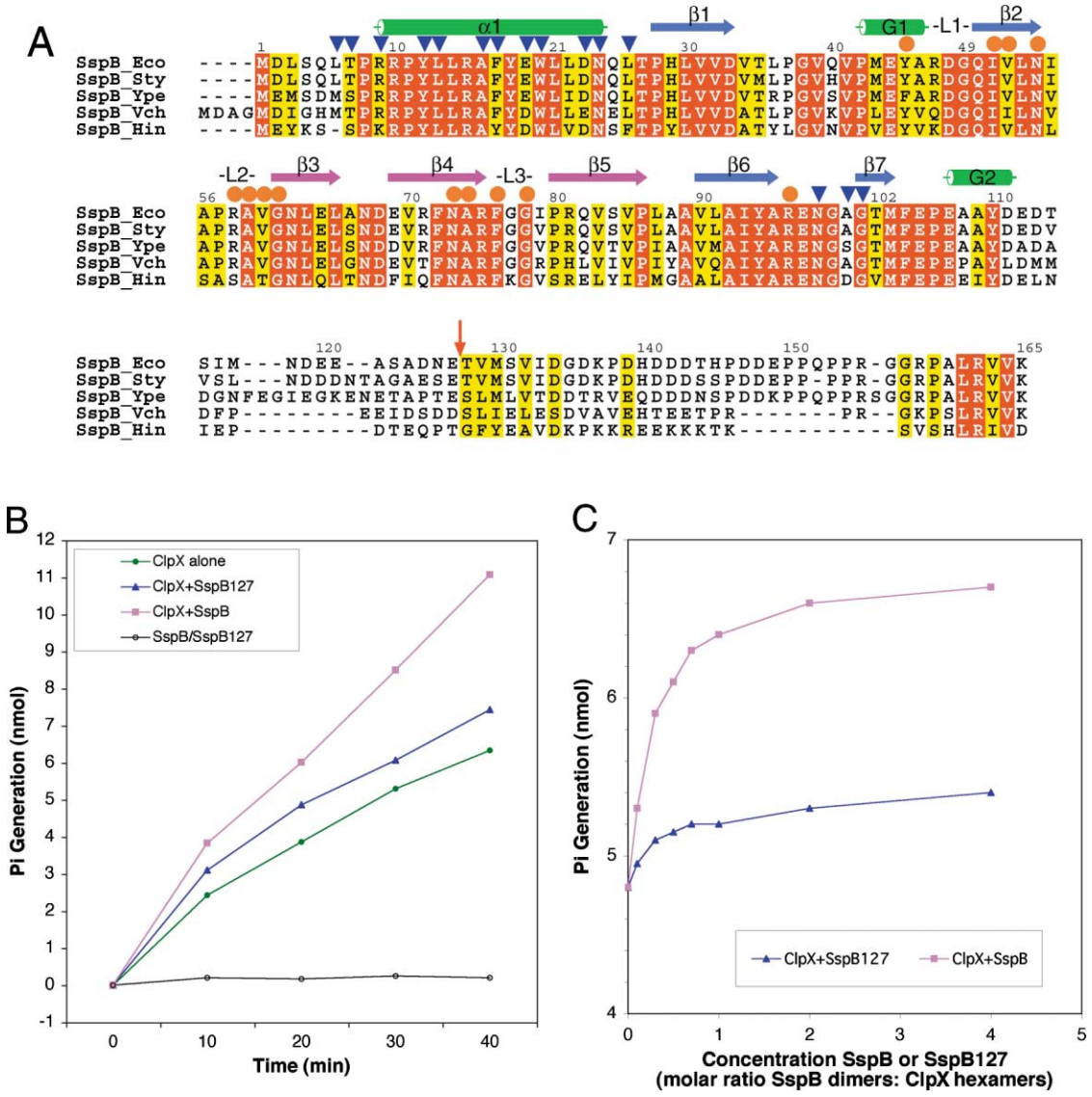

Figure 2. SspB Sequence Alignment and the Effect of SspB on the ATPase Activity of ClpX

(A) Sequence alignment of SspB proteins from *Escherichia coli* (Eco), *Salmonella typhimurium* (Sty), *Yersinia pestis* (Ype), *Vibrio cholerae* (Vch), and *Haemophilus influenzae* (Hin). Secondary structure elements are indicated above the sequence and colored as in Figure 3. The three loops (L1, L2, and L3) that contribute to the SsrA binding pocket are also labeled. Key residues involved in dimerization are marked with blue triangles. Orange circles indicate residues involved in SsrA recognition. The terminal residue of SspB127 construct is marked by a red arrow. Shading indicates residues that are identical (red) or highly conserved (yellow) in all sequences.

(B) ATP hydrolysis was assayed by incubating 2.5 μg of ClpX and 2 mM ATP in the absence (green circles) and presence of 1:1 molar ratio of SspB (magenta squares) or SspB127 (blue triangles) for various time periods at 37°C. SspB and SspB127 alone (open black circles) have no ATPase activity.

(C) The assays were also performed as (B) but by incubating ClpX for 20 min in the presence of increasing amounts of SspB (magenta squares) or SspB127 (blue triangles). Note that addition of one full-length SspB dimer per ClpX hexamer almost fully activates the ClpX ATPase and that addition of the truncated SspB127 protein yields minimal activation.

(A) was drawn with ALSCRIPT (Barton, 1993).

and therefore toxic to the cell because they are prone to aggregation. Association of SspB with the ribosome might facilitate binding of these aborted polypeptides prior to their release into the cytoplasm in much the same way that the ribosome-associated chaperone TF (trigger factor) sequesters nascent polypeptides under normal conditions (Bukau et al., 2000). The present structure will facilitate structure/function studies of ribosome recognition by SspB.

The SspB dimer interface is formed largely by interactions between the 25 Å long N-terminal α helix (α1) in each dyad-related molecule. The 2-fold related helices are roughly antiparallel (Figure 3A), and residues Leu6, Thr7, Arg9, Tyr12, Leu13, Ala16, Phe17, Glu19, Trp20, Asp23, Asn24, and Leu26 in each helix participate in the dimer interface (Figure 2A). Additionally, residues Asn98, Ala100, and Gly101 (in the loop preceding strand β7) contribute to the mostly hydrophobic interaction. We

Table 1. Data Collection and Refinement Statistics

	Free SspB127 (MAD)			
Data collection	Peak	Edge	Remote	Full-Length SspB-SsrA Complex
Wavelength (Å)	0.9785	0.9791	0.9500	0.9500
Resolution (Å) (outer shell)[a]	2.2 (2.2–2.26)	2.2 (2.2–2.26)	2.2 (2.2–2.26)	2.9 (2.9–2.99)
Space group		$P4_32_12$		$P2_1$
Unit cell parameters (Å, °)		a = b= 60.12, c = 187.98		a = 81.51, b = 81.53, c = 131.77, β = 92.83
Number of mols /A.S.U.		2		8 (SspB), 8 (SsrA)
Total reflections	503,846	501,858	203,874	86,232
Unique reflections	18,454	18,481	18,430	34,398
Completeness (%)[a]	100.0 (100.0)	100.0 (100.0)	99.7 (99.7)	93.4 (89.9)
R_{merge} (%)[a,b]	6.5 (19.6)	5.4 (19.3)	6.4 (31.7)	12.4 (23.6)
Figure of merit[c]		0.56 for 15-2.6 Å		
Refinement				
Resolution range (Å)		30–2.2		30–2.9
Number of reflections		16,749		34,270
R_{work}/R_{free} (%)[d]		24.9/28.4		24.5/29.7
Number of modeled residues				
Protein (SspB)		2 × 107 (Q5-D111)		8 × 108 (S4-D111)
Peptide (SsrA)		–		8 × 8 (A1-A8)
Number of atoms				
Protein/peptide/water		1,697/–/114		6,792/488/–
Rms bond length (Å)		0.006		0.008
Rms bond angles (°)		1.38		1.43
Estimated coordinate error (Å)		0.36		0.39
Average B value (Å^2)				
Main/side chain		47.4/49.7		25.7/27.3
Peptide/water		–/49.8		32.0/–

[a] Values in parentheses are for reflections in the highest resolution bin.
[b] $R_{merge} = \Sigma_h\Sigma_i|I(h,I) - \langle I(h)\rangle|/\Sigma_h\Sigma_i\, I(h,i)$, where I(h,i) is the intensity of the i^{th} measurement of h and $\langle I(h)\rangle$ is the corresponding average value for all i measurements.
[c] Figure of merit $= |\Sigma P(\alpha)e^{i\alpha}/\Sigma P(\alpha)|$, where $P(\alpha)$ is the phase probability distribution and α is the phase.
[d] R_{work} and $R_{free} = \Sigma||F_O|-|F_C||/\Sigma|F_O|$ for the working set and test set (10%) of reflections.

observe hydrogen bond interactions between Asp23 and Tyr12 in 2-fold related molecules, and water-mediated hydrogen bonds between Thr7 and Tyr12 and between Arg9 and Asn101. The solvent-accessible surface area buried in the interface is ~730 Å^2 per monomer (http://www.biochem.ucl.ac.uk/bsm/PP/server/), well within the expected range for a stable dimer association (Jones and Thornton, 1996).

The SsrA peptide binds in a hydrophobic groove formed by one edge of the β sandwich and by the L1, L2, and L3 loops. The SsrA binding groove is approximately perpendicular to the N-terminal helix and parallels the 2-fold symmetry axis of the dimer. Thus, the two SsrA tags bound by the SspB dimer are parallel to one another and run in the same direction from their N to C termini (into the plane of the page, as shown in the left panel of Figure 3A). As discussed below, this symmetry suggests a general mode of association with the ClpXP degradation machine.

SsrA Recognition

In our complex structure, the SsrA peptide binds in an irregular conformation in a groove formed by strand β2 and by loops L1, L2, and L3 (Figure 5). We are able to build the first 8 residues (AANDENYA) of the 11 residue SsrA tag (Figure 3C); 6 of these 8 residues appear to make key specificity-determining interactions with SspB. The disorder of the C-terminal SsrA residues is not unexpected, as exhaustive mutational studies of the SsrA tag have indicated that residues 9–11 of SsrA interact with ClpX, whereas residues 1–4 and 7 bind SspB (Flynn et al., 2001).

SsrA binding is stabilized by numerous hydrophobic and hydrogen bond interactions involving both the peptide backbone and side chains (Figure 5A). Alanine appears to be favored in the first two positions [alanines 1(p) and 2(p); for clarity we use "(p)" to designate residue in the SsrA peptide] as these side chains extend into shallow hydrophobic depressions that would not readily accommodate bulkier groups. Asn3(p) in the peptide is highly conserved and makes critical buried hydrogen bond interactions with the backbone amide and carbonyl groups of Asn54 in SspB. Asparagine is likely required in this position of SsrA because no other residue could be accommodated and contribute both hydrogen bonds without considerable structural rearrangements. Asp4(p) hydrogen bonds with a backbone amide in loop L2, while Glu5(p) extends into a basic pocket formed by arginines 58 and 96 (Figure 5C). These well-conserved residues may contribute electrostatic stabilization to the complex. For example, the guanidinium moiety of Arg96 and carboxylic side chain of Glu5(p) form a salt bridge (<3.5 Å) in five of the eight SspB-SsrA complexes in the asymmetric unit. Peptide array studies indicate that substitutions are tolerated at this position (Wah et al., 2002); the structure shows that other residues can be

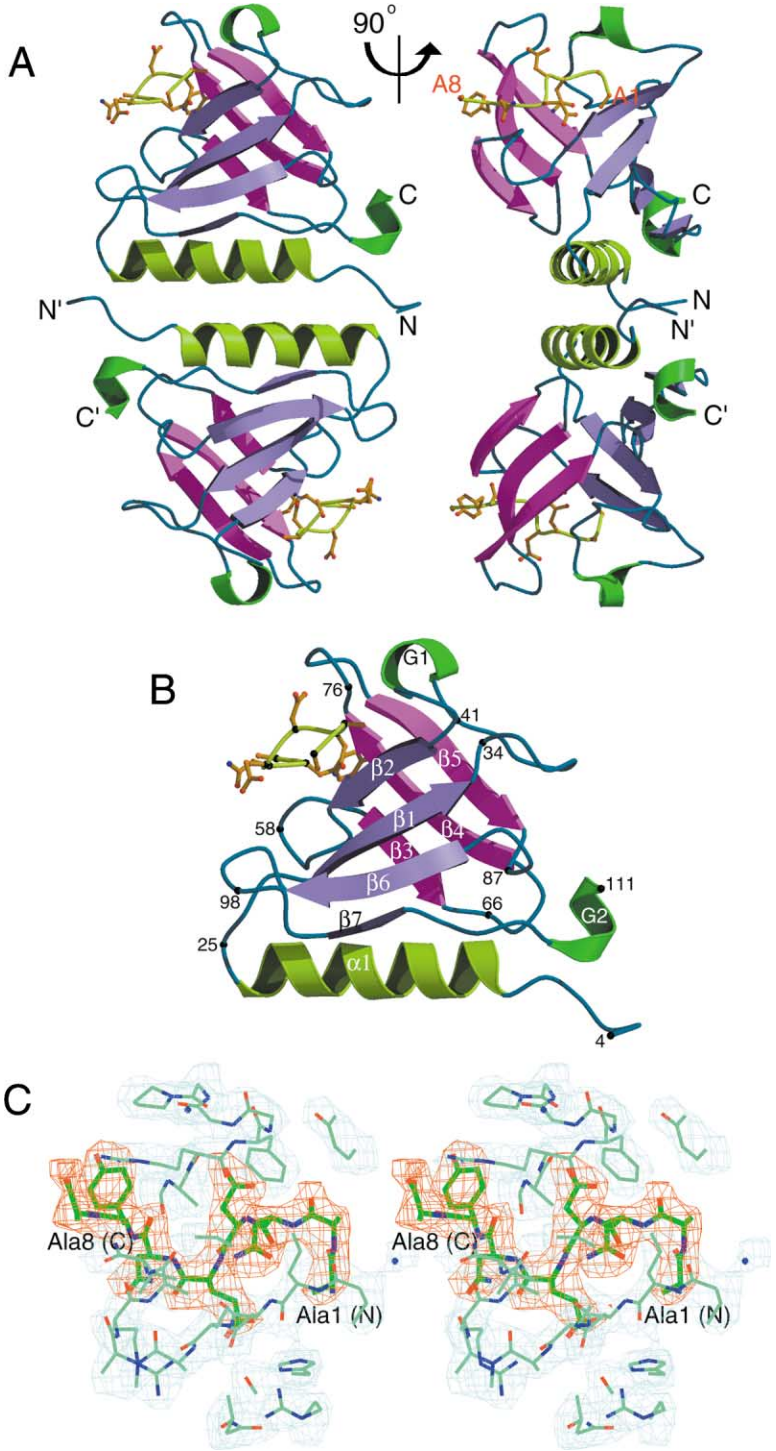

Figure 3. Structure of the SspB/SsrA Complex

(A) Ribbon diagram showing the dimeric SspB/SsrA complex structure viewed along the noncrystallographic 2-fold molecular symmetry axis (left). Secondary structural elements are colored light green (N-terminal α helix), dark green (two 3_{10} helices), slate (front β sheet), purple (back β sheet), and light blue (connecting loops). The bound SsrA peptide is also shown (yellow). The view in the right panel is rotated by 90° as indicated. The N and C termini of SspB are labeled, as are the first and last residues of the SsrA tag (A1 and A8).

(B) Ribbon diagram showing the secondary structure elements of the SspB monomer. Approximately every tenth residue is labeled and marked by a black dot. G1 and G2 indicate two segments of 3_{10} helix.

(C) Stereo view of electron density maps showing the bound SsrA peptide and its binding site in SspB. The $|F_o - F_c|$ map (orange color) was calculated prior to inclusion of the illustrated SsrA peptide residues in the model. This map was calculated using 30–2.9 Å data and is contoured at 2.5 σ. The $|2F_o - F_c|$ map (sky blue color) corresponding to SspB model was calculated using 30–2.9 Å data and is contoured at 1.0 σ.

(A) and (B) were drawn with MOLSCRIPT (Kraulis, 1991) and rendered with RASTER 3D (Merritt and Bacon, 1997). (C) was prepared with CHAIN (Sack, 1988).

sterically accommodated but that glutamic acid may be favored for electrostatic reasons. Tyr7(p) makes numerous van der Waals interactions in a cleft flanked by the side chains of Asn73 and Arg75. C-terminal to Tyr7(p), the SsrA backbone extends away from SspB, presumably allowing engagement of its C-terminal residues by ClpX. The SspB/SsrA interaction buries a total of ~1180 Å^2 of solvent-accessible surface (http://www.biochem.ucl.ac.uk/bsm/PP/server/). Additional interactions are presented in Figure 5. Sequences of the tmRNA encoding the SsrA tag have been reported for over 260 species across 17 phyla (the tmRNA site, http://www.indiana.edu/~tmrna/); a large subset of these preserve the A-A-N-D-E/D-x-Y/F motif bound by SspB. Additionally, the SsrA peptide recognition site in SspB is conserved in a wide range of prokaryotes (Figure 2A).

Comparison of the free and SsrA-bound SspB structures reveals little conformational change upon binding

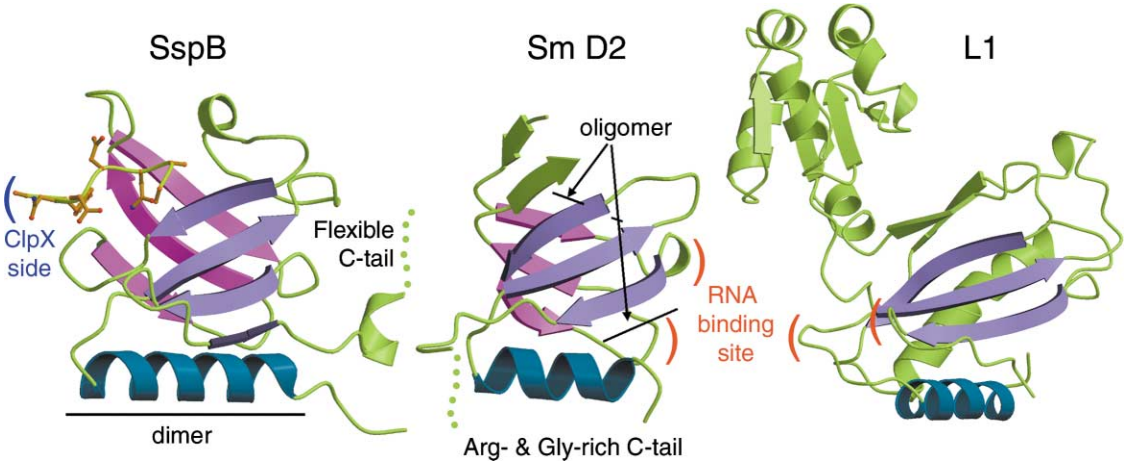

Figure 4. SspB Shares Structural Homology with RNA Binding Proteins

Ribbon diagrams comparing the overall structures of SspB, Sm D2, and ribosomal protein L1 are shown in a similar orientation. Structurally related regions of the three molecules are colored blue and purple while structurally divergent parts are drawn in green. For SspB, the dimer contact region, flexible C-terminal tail, and hypothesized ClpX binding region are indicated. The regions involved in the oligomerization of Sm D2 are marked, as are the RNA binding sites in Sm D2 and L1. Although the C-terminal tail of Sm D2 has no distinct arginine- and glycine-rich sequence, the homologous proteins Sm D1, D3, and B have unstructured arginine- and glycine-rich tails that are involved in protein-protein interactions. Note that the oligomerization interfaces are not conserved between SspB and Sm proteins, nor are the RNA interaction sites in Sm D2 and L1.

of the degradation tag (Figure 5B). The rms deviation between free and SsrA-complexed states is 0.67 Å for all Cα atoms. The most significant rearrangements occur in loops L1 and L3, which flank the bound SsrA peptide (Figure 5B). Average main chain displacements in loops L1 (residues 42–49) and L3 (residues 74–80) are 1.2 and 1.6 Å, respectively.

Interestingly, we observe a long hydrophobic channel on the surface of SspB (Figure 5D). The SsrA peptide occupies one end of the channel, where it is flanked by basic residues, but the more hydrophobic portion of the channel extends well beyond the N terminus of SsrA (Figure 5D). Many molecular chaperone/unfoldase proteins are known to utilize hydrophobic patches to form transient complexes with hydrophobic residues exposed in nonnative peptides (Hartl, 1996; Bukau and Horwich, 1998). This channel is well positioned to interact with residues of an unfolded (or unfolding) substrate adjacent to the SsrA tag. As noted above, SspB may have higher affinity for SsrA-tagged substrate proteins than for the isolated tag (Wah et al., 2002). Thus, we propose that authentic SsrA-tagged substrates, which may have misfolded/unfolded regions adjacent to the C-terminal SsrA tag, may bind transiently in this channel during unfolding and degradation. Mutation of key residues in the channel, including Val31, Leu91, and Met103, will allow a test of this hypothesis.

Insight into Interaction with ClpX

SspB is essential for delivery of SsrA-marked protein substrates to ClpXP. In contrast to the activity of ClpAP on globally unfolded substrates, ClpXP is unable to degrade denatured proteins without the SsrA tag (Hoskins et al., 2000). ClpX alone can recognize only the C-terminal three residues (LAA) of SsrA tag (Flynn et al., 2001), which provides insufficient specificity as there are number of proteins bearing C-terminal LAA sequence that are not ClpXP substrates. Moreover, GFP tagged with SsrA mutants retaining only the LAA sequence are not degraded efficiently by ClpXP (Flynn et al., 2001). Thus, SspB is a crucial specificity-enhancing factor for recognition of SsrA-marked proteins by ClpXP.

How might SspB associate with ClpX and feed SsrA-tagged polypeptides into ClpP? EM studies of substrate translocation show that substrate is recognized on the distal face of the ClpX molecule—the face opposite the ClpP contact region (Figure 6B) (Ortega et al., 2000). In contrast to ClpA (Guo et al., 2002b) and HslU (ClpY) (Bochtler et al., 2000; Sousa et al., 2000; Wang et al., 2001), no atomic structure for ClpX is available so far, but the sequence similarity between ClpX and HslU allows us to model ClpX, except for an N-terminal region of ~60 amino acid residues in ClpX which is known as C4-type zinc finger (Banecki et al., 2001). Interestingly, ClpX has no I domain between its N and C domains; the I domain has been shown to be a substrate recognition domain in HslU (Song et al., 2000). Figure 6 shows the homology model of ClpX and its comparison with HslU. Because it has no equivalent in HslU, we could not model the N-terminal zinc finger domain. Instead, we represent this domain with transparent ovals (Figure 6B) positioned as suggested by EM images of ClpX (Grimaud et al., 1998). It is unclear whether the N-terminal zinc finger domain of ClpX is actively involved in the SspB interaction, but it seems likely given that many adaptor proteins for AAA+ ATPases use a divergent N-terminal domain of the ATPase to bind and modulate activity (Dougan et al., 2002a).

The structural considerations outlined above, together with the observed dimer:hexamer stoichiometry of the SspB:ClpX interaction, suggest a possible mode of association in which the 2-fold axis of SspB is aligned with the 6-fold axis of ClpX (Wah et al., 2002), and the

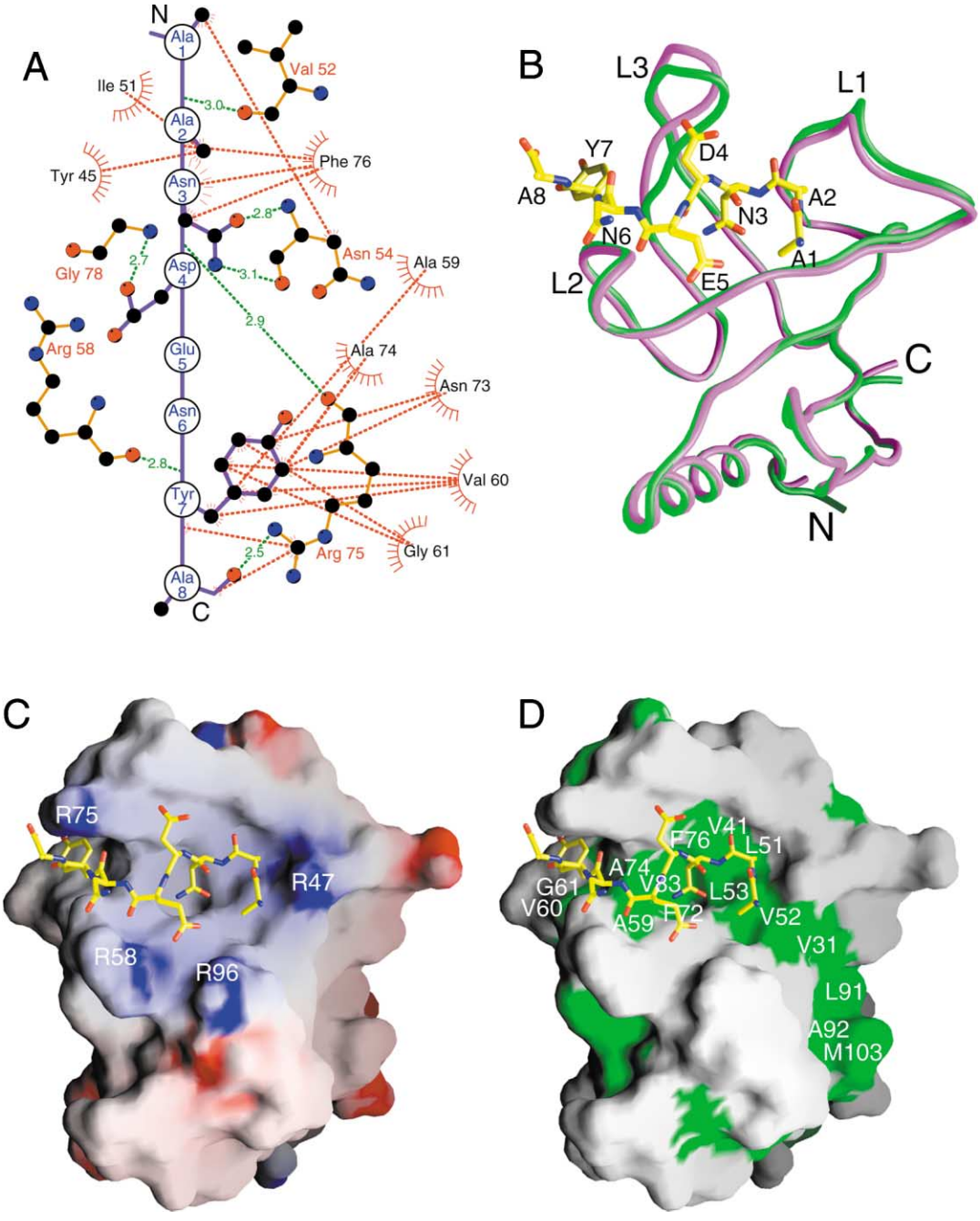

Figure 5. SsrA-Peptide Binding Site of SspB

(A) Schematic diagram showing interactions between SspB and the SsrA peptide. Hydrophobic interactions are denoted by red starbursts and dashed lines; hydrogen bonding interactions by green dashed lines.

(B) Backbone superposition of free (magenta) and SsrA complex (green) structure. N and C termini of SspB and the regions showing a significant structural movement (L1 and L3) are labeled. Bound SsrA peptide is also drawn and labeled.

(C) Electrostatic surface representation of SspB. Negatively charged regions are red and positively charged regions blue.

(D) Hydrophobic surface representation of SspB. Residues forming the hydrophobic surfaces of SspB are colored green and labeled. Note the extended hydrophobic channel that extends beyond the SsrA binding region.

The view for (B), (C), and (D) is similar to Figure 2A, right. (A) was drawn with LIGPLOT (Wallace et al., 1995), and (B), (C), and (D) were drawn with GRASP (Honig and Nicholls, 1995).

SspB dimer is oriented such that the C terminus of the SsrA tag extends toward ClpX (Figures 6B and 6C). These considerations restrict the relative orientation of SspB and ClpX in two of three rotational dimensions. The remaining dimension, corresponding to rotation about the dyad axis, is not restrained but could vary

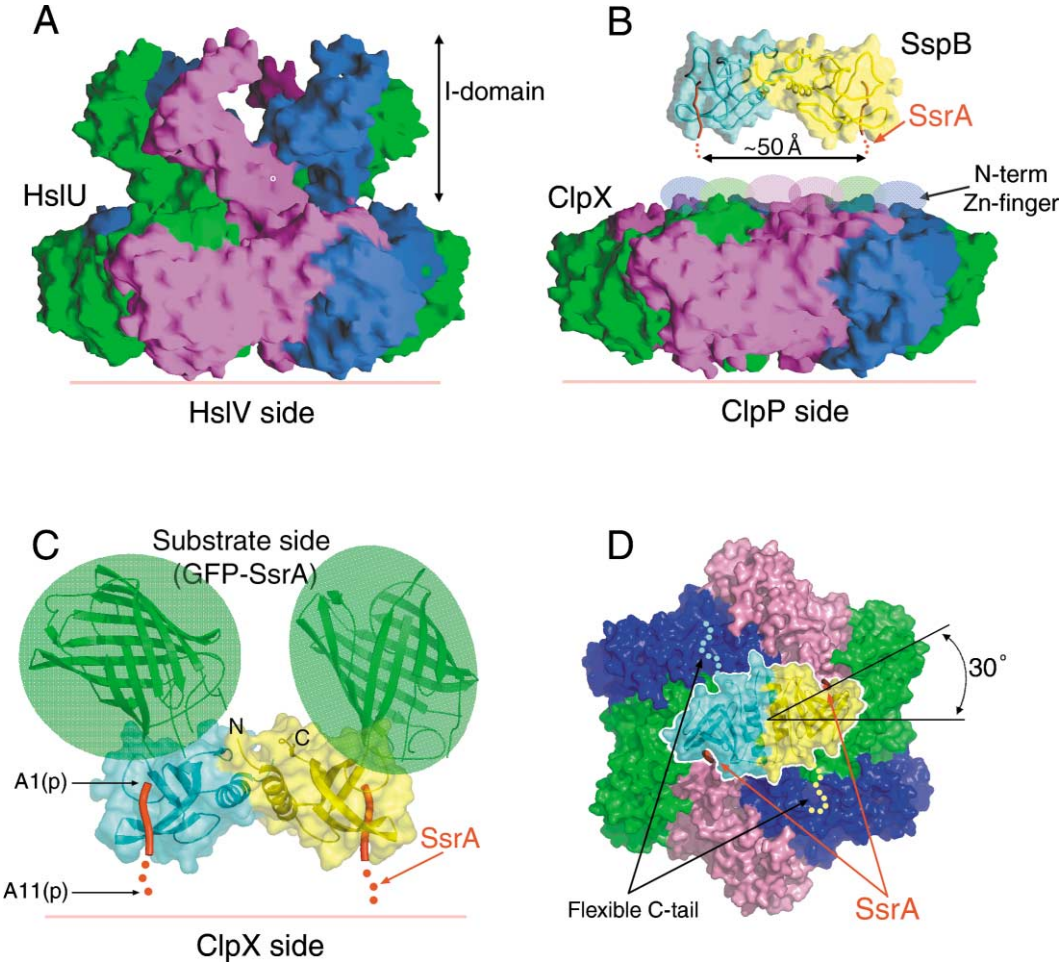

Figure 6. A Proposed Mode of Interaction of the SspB/SsrA Complex with ClpX

(A) A side view of HslU molecule with the I domain extending upward. The three dimers in the hexamer are colored green, magenta, and blue. The side of HslU that binds the HslV protease is marked, and the position of the I domain is indicated.

(B) The ClpX homology model is shown with the same view and color scheme (see text). Transparent ovals represent the N-terminal zinc finger domain that is not otherwise modeled. The exact location of this domain in the ClpX hexamer and the physical interaction with SspB are not clear. The side of ClpX that interacts with the ClpP protease is marked. SspB is shown above ClpX as a transparent molecular surface over a ribbon model. In the orientation shown, the SsrA peptides are positioned to thread into ClpX. The distance between the bound SsrA peptides, which will in part anchor SspB to ClpX, is approximately 50 Å (roughly the same as the distance between the insertion points in the HslU I domain.

(C) Orientation of SsrA-tagged substrates in the SspB dimer. Green fluorescent protein, a model substrate, is shown as transparent ovals over ribbon diagrams of GFP to illustrate the relative orientation of substrates. As illustrated here, GFP is on the side of SspB distal to ClpX, and the SsrA tag extends toward ClpX. The last three residues of SspB, which are known to be required for ClpXP binding, are unstructured here and are shown as red dots. Although the exact orientation of substrates is ambiguous, their position is distal to ClpX based on the orientation of bound SsrA peptide.

(D) Top view (90° rotation of [B] along the horizontal axis) showing the proposed orientation of dimeric SspB with respect to hexameric ClpX. Although the exact orientation is ambiguous, symmetry restraints constrain the relative position of SspB to within 30°. The flexible C-terminal tail of SspB may also participate in docking with ClpX.

(A) and (B) were drawn with GRASP (Honig and Nicholls, 1995), and (C) and (D) were drawn with PyMOL (http://pymol.sourceforge.net/).

over a 30 degree range (the interaction of the 2-fold symmetry of SspB and the 6-fold symmetry of ClpX means that the interactions will be identical after any 30 degree rotation). This arrangement would position the SspB subunits for symmetric interactions with ClpX protomers on opposite sides of the hexamer, and orient both bound SsrA tags for recognition by ClpX. Additionally, the hydrophobic channel of each SspB monomer is exposed for putative interaction with unfolded substrates. Note also that this 2:6 mode of association could break the 6-fold symmetry of ClpX and that it could effect an ATPase reaction cycle because SspB enhances ATPase activity (Figure 2B). The axial positioning of the I domain in HslU and the similar mode of association of SspB with ClpX that we propose is distinctly different from the lateral mode of association of proposed for ClpS with ClpA. In recent structures of the N-terminal domain of ClpA in complex with the specificity-enhanc-

ing factor ClpS, the ClpS protein is proposed to extend to the side of the ClpA hexamer (Guo et al., 2002a; Zeth et al., 2002). An unambiguous understanding of the mode of association of SspB and ClpX will require structural analysis of a complex.

Experimental Procedures

Sample Preparation

The *sspB* gene was cloned using standard polymerase chain reaction (PCR) techniques. PCR primers were designed based on the reported *E. coli* genomic DNA sequences (Blattner et al., 1997). The *sspB* was flanked by NdeI and BamHI restriction enzyme sites. The resultant fragments were ligated into pET-12b expression vectors (Novagen). The integrity of the resultant plasmids was verified by DNA sequencing. The plasmids were then transformed into BL21(DE3) cells. Expression of cloned genes was induced by the addition of 1 mM IPTG at OD (600 nm) = 0.6. The cells were centrifuged and kept frozen at −80°C until further use. C-terminal truncated version of SspB, SspB127 (residues 1–127), was cloned and expressed by the same procedure as described above. Recombinant SspB and its variant were purified by the reported procedure with minor modification (Levchenko et al., 2000). The cell pellet was resuspended in ice-cold buffer A (50 mM Tris-HCl [pH 7.7], 100 mM NaCl, 1 mM EDTA, 2 mM β-mercaptoethanol) and subsequently disrupted by ultrasonication. The proteins were fractionated by ammonium sulfate precipitation (20%–35%) and then dialyzed against buffer A extensively. The dialysate containing target protein was loaded onto a Hi-Trap Q-Sepharose anion exchange column (5 ml, Amersham-Pharmacia) and further purified by gel filtration (Superdex 75, Amersham-Pharmacia). Selenomethionyl SspB127 was expressed with BL21(DE3) cells using the inhibition of methionine biosynthesis (Doublies, 1997) and purified as wild-type protein. The N-terminal sequencing and electron spray ionization mass spectroscopic (ESI-MS) analyses were carried out to check the integrity of the purified protein samples.

N-terminal histidine-tagged GFP-SsrA (His-GFP-SsrA) in vector pTrc99A was a gift of Drs. P. Zwickl and T. Tamura. The *clpX* and *clpP* genes were cloned using standard PCR techniques with genomic DNA as a template. They were cloned into the His-tag containing vectors. A similar procedure was used to purify ClpX, ClpP, and GFP-SsrA, except that the Ni-NTA column was used for the first step instead of ammonium sulfate fractionation. Proteins were quantified by their absorbance at 280 nm or by the method of Bradford using bovine serum albumin as a standard. ATPase activity was measured by determining the amount of inorganic phosphate formed on ATP hydrolysis and detected at 660 nm as a complex with malachite green and ammonium molybdate (Lanzetta et al., 1979).

Limited Proteolysis

For preparative proteolysis, 1 mg/ml of SspB protein solution in 50 mM Tris-HCl (pH 7.7) and 250 mM NaCl was mixed with 1 mg/ml of various classes of protease including trypsin, chymotrypsin, papain, carboxypeptidases A, B, and Y, elastase, subtilsin, and GluC-endopeptidase in 50 mM Tris-HCl (pH 8.0) in a 100:1 (v/v) ratio. The solution was incubated for several minutes to hours at room temperature. To stop the reaction, equal volume of SDS-PAGE buffer was added and boiled immediately. The digestion products were separated and visualized by SDS-PAGE; selected bands were further analyzed by N-terminal sequencing and mass spectrometry.

Histidine-Tag Pull-Down Assay with Purified His-GFP-SsrA and SspB

His-GFP-SsrA protein was loaded onto the nickel-NTA column equilibrated with 50 mM Tris-HCl (pH 8.0), 100 mM NaCl, and then the beads in the column were incubated with an approximate 2- to 3-fold molar excess of SspB or SspB127 for 30 min at 4°C. After washing the nonspecific binding proteins from the nickel-NTA column with 50 mM imidazole extensively, the bound proteins were eluted with 300 mM imidazole. Eluents were analyzed by SDS-PAGE and visualized with Coomassie blue stain.

Circular Dichroism Spectroscopy

CD spectra were recorded at 4°C on an Aviv 62DS spectropolarimeter equipped with a thermoelectric temperature controller. SspB or SspB127 (50 μM, calculated as a monomer) was prepared in 20 mM phosphate (pH 7.4) and 100 mM NaCl. Spectra representing the average of five scans from 260 to 195 nm were measured in a 1 mm path length cuvette using a step size of 1 nm and a 3 s signal-averaging time. All spectra were corrected for the baseline by substracting reference spectra of buffer alone.

Isothermal Titration Calorimetry

Experiments were performed using the MSC system (MicroCal Inc.) The SspB (or SspB127) protein was diluted to a concentration of 50 μM in the ITC buffer (50 mM Tris-HCl [pH 7.7], 100 mM NaCl) and placed in the sample cell. SsrA peptide was diluted, and His-GFP-SsrA protein was concentrated to a final concentration of 500 μM in the ITC buffer and placed in the injection syringe. In each titration experiment, 30 aliquots of SsrA peptide or His-GFP-SsrA (10 μl each) was injected under computer control into the 1.3 ml sample cell at 25°C. The experimental data were corrected for dilution by subtracting the curve obtained by titration into buffer alone and then fit by least squares regression assuming a one-site binding model using the ORIGIN software provided with the instrument.

Crystallization and Data Collection

The purified SspB (or SspB127) was concentrated to 25 mg/ml in 50 mM Tris-HCl (pH 7.7), 250 mM NaCl, 2 mM EDTA, and 2 mM β-mercaptoethanol. Crystallization was performed by the hanging-drop vapor diffusion method at 22°C. For SspB/SsrA complex crystallization, a 10-fold molar excess of solid SsrA peptide (AANDENYALAA) was added and incubated overnight at 4°C. Insoluble material was removed by centrifugation immediately prior to crystallization. The complex between SspB and the SsrA peptide was crystallized within several days over a reservoir of 100 mM sodium cacodylate (pH 6.5), 200 mM magnesium acetate, and 15%–18% polyethylene glycol 8000. Data were collected on a charge-coupled device detector at the F1 beamline of the Cornell High Energy Synchrotron Source, Cornell University. Diffraction data were processed and scaled using the DENZO/SCALEPACK (Otwinowski and Minor, 1997).

The reservoir solution for crystallization of the SspB127 protein (native and Se-Met substituted) consisted of 100 mM HEPES-KOH (pH 7.5) containing 4.0–4.1 M NaCl. For cryocooling, a crystal was transferred to reservoir solution containing increased NaCl concentration (4.2 M) before flash-freezing in a nitrogen stream at 100 K. Diffraction data were collected on a charge-coupled device detector at the X12C beamline of the National Synchrotron Light Source, Brookhaven National Laboratory. Diffraction data were processed and scaled using the HKL2000 software package (Otwinowski and Minor, 1997).

Structure Determination and Refinement

Four of eight possible selenium sites (including two N-terminal methionine residues) in the SspB127 asymmetric unit were located with SOLVE (Terwilliger and Berendzen, 1999). The phases were improved with DM (CCP4, 1994). The electron density was of sufficient quality to identify and build the long N-terminal α helices. Using a partial model including these helices and the selenium sites, the noncrystallographic symmetry operators were calculated. Subsequent 2-fold NCS averaging with DM yielded an excellent electron density map that allowed construction of a nearly complete model. The model was rebuilt with the program O (Jones et al., 1991). The protein model was refined with CNS (Brunger et al., 1998), including the bulk solvent correction. The 2-fold noncrystallographic symmetry was maintained with tight restraint during the early stages of refinement but was relaxed in the final rounds. The model of SspB127 (Se-Met substituted) accounts for 107 residues in both subunits, and no electron density was observed for the C-terminal tail (Table 1). Solvent molecules were added using model-phased difference Fourier maps by using CNS (Brunger et al., 1998). Statistics for the refined model are presented in Table 1.

Phases of SspB-SsrA complex crystal were obtained by molecular replacement with the program MOLREP (Vagin and Teplyakov, 2000) using refined dimeric SspB127 as a search model. Refinement of

the model was performed as above to a final R value of 24.5% (R_{free} = 29.7%). These relatively high R factors are likely a consequence of the large number of unstructured residues in the complex structure (we observe no interpretable electron density for 57 residues in each of the eight molecules in the asymmetric unit). The positions of the SsrA peptide were clearly determined by using model-phased difference Fourier map contoured at 2.5 σ. The assesssment of model geometry and the assignment of secondary structure elements were done with the program PROCHECK (Laskowski et al., 1993).

Acknowledgments

We thank Dr. P.W. Kim for assistance with the ITC experiments and the staff at F1 beamline, MacCHESS and X12C beamline, NSLS, BNL for help with data collection. We also thank Drs. P. Zwickl (Max-Planck-Institute for Biochemistry, Germany) and T. Tamura (National Institute of Advanced Industrial Science and Technology, Japan) for cells containing His-GFP-SsrA and Prof. R. Huber for his generous support in the initial stage of this project. This work was supported in part by a grant from the National Institutes of Health (M.J.E.). M.J.E. is a recipient of a Scholar Award from the Leukemia and Lymphoma Society.

Received: March 5, 2003
Revised: May 6, 2003
Accepted: May 19, 2003
Published: July 24, 2003

References

Banecki, B., Wawrzynow, A., Puzewicz, J., Georgopoulos, C., and Zylicz, M. (2001). Structure-function analysis of the zinc-binding region of the ClpX molecular chaperone. J. Biol. Chem. *276*, 18843–18848.

Barton, G.J. (1993). ALSCRIPT: A tool to format multiple sequence alignments. Protein Eng. *6*, 37–40.

Blattner, F.R., Plunkett, G., 3rd, Bloch, C.A., Perna, N.T., Burland, V., Riley, M., Collado-Vides, J., Glasner, J.D., Rode, C.K., Mayhew, G.F., et al. (1997). The complete genome sequence of *Escherichia coli* K-12. Science *277*, 1453–1474.

Bochtler, M., Hartmann, C., Song, H.K., Bourenkov, G.P., Bartunik, H.D., and Huber, R. (2000). The structures of HslU and the ATP-dependent protease HslU-HslV. Nature *403*, 800–805.

Brunger, A.T., Adams, P.D., Clore, G.M., DeLano, W.L., Gros, P., Grosse-Kunstleve, R.W., Jiang, J.S., Kuszewski, J., Nilges, M., Pannu, N.S., et al. (1998). Crystallography & NMR system: A new software suite for macromolecular structure determination. Acta Crystallogr. D *54*, 905–921.

Bukau, B., and Horwich, A.L. (1998). The Hsp70 and Hsp60 chaperone machines. Cell *92*, 351–366.

Bukau, B., Deuerling, E., Pfund, C., and Craig, E.A. (2000). Getting newly synthesized proteins into shape. Cell *101*, 119–122.

CCP4 (Collaborative Computational Project 4) (1994). The CCP4 suite: programs for protein crystallography. Acta Crystallogr. D *50*, 760–763.

Conaway, R.C., Brower, C.S., and Conaway, J.W. (2002). Emerging roles of ubiquitin in transcription regulation. Science *296*, 1254–1258.

Doublies, S. (1997). Preparation of selenomethionyl proteins for phase determination. In Methods in Enzymology, C.W. Carter, Jr., and R.M. Sweet, eds. (New York: Academic Press), pp. 523–530.

Dougan, D.A., Mogk, A., Zeth, K., Turgay, K., and Bukau, B. (2002a). AAA+ proteins and substrate recognition, it all depends on their partner in crime. FEBS Lett. *529*, 6–10.

Dougan, D.A., Reid, B.G., Horwich, A.L., and Bukau, B. (2002b). ClpS, a substrate modulator of the ClpAP machine. Mol. Cell *9*, 673–683.

Flynn, J.M., Levchenko, I., Seidel, M., Wickner, S.H., Sauer, R.T., and Baker, T.A. (2001). Overlapping recognition determinants within the SsrA degradation tag allow modulation of proteolysis. Proc. Natl. Acad. Sci. USA *98*, 10584–10589.

Gillet, R., and Felden, B. (2001). Emerging views on tmRNA-mediated protein tagging and ribosome rescue. Mol. Microbiol. *42*, 879–885.

Gottesman, S., Maurizi, M.R., and Wickner, S. (1997). Regulatory subunits of energy-dependent proteases. Cell *91*, 435–438.

Gottesman, S., Roche, E., Zhou, Y., and Sauer, R.T. (1998). The ClpXP and ClpAP proteases degrade proteins with carboxy-terminal peptide tails added by the SsrA-tagging system. Genes Dev. *12*, 1338–1347.

Grimaud, R., Kessel, M., Beuron, F., Steven, A.C., and Maurizi, M.R. (1998). Enzymatic and structural similarities between the Escherichia coli ATP-dependent proteases, ClpXP and ClpAP. J. Biol. Chem. *273*, 12476–12481.

Guo, F., Esser, L., Singh, S.K., Maurizi, M.R., and Xia, D. (2002a). Crystal structure of the heterodimeric complex of the adaptor, ClpS, with the N-domain of the AAA+ chaperone, ClpA. J. Biol. Chem. *277*, 46753–46762.

Guo, F., Maurizi, M.R., Esser, L., and Xia, D. (2002b). Crystal structure of ClpA, an Hsp100 chaperone and regulator of ClpAP protease. J. Biol. Chem. *277*, 46743–46752.

Hartl, F.U. (1996). Molecular chaperones in cellular protein folding. Nature *381*, 571–579.

Hayes, C.S., Bose, B., and Sauer, R.T. (2002a). Proline residues at the C terminus of nascent chains induce SsrA tagging during translation termination. J. Biol. Chem. *277*, 33825–33832.

Hayes, C.S., Bose, B., and Sauer, R.T. (2002b). Stop codons preceded by rare arginine codons are efficient determinants of SsrA tagging in *Escherichia coli*. Proc. Natl. Acad. Sci. USA *99*, 3440–3445.

Hershko, A., and Ciechanover, A. (1998). The ubiquitin system. Annu. Rev. Biochem. *67*, 425–479.

Honig, B., and Nicholls, A. (1995). Classical electrostatics in biology and chemistry. Science *268*, 1144–1149.

Hoskins, J.R., Singh, S.K., Maurizi, M.R., and Wickner, S. (2000). Protein binding and unfolding by the chaperone ClpA and degradation by the protease ClpAP. Proc. Natl. Acad. Sci. USA *97*, 8892–8897.

Jones, S., and Thornton, J.M. (1996). Principles of protein-protein interactions. Proc. Natl. Acad. Sci. USA *93*, 13–20.

Jones, T.A., Zou, J.-Y., Cowan, S.W., and Kjeldgaard, M. (1991). Improved methods for binding protein models in electron density maps and the location of errors in these models. Acta Crystallogr. A *47*, 110–119.

Kambach, C., Walke, S., Young, R., Avis, J.M., de la Fortelle, E., Raker, V.A., Luhrmann, R., Li, J., and Nagai, K. (1999). Crystal structures of two Sm protein complexes and their implications for the assembly of the spliceosomal snRNPs. Cell *96*, 375–387.

Keiler, K.C., Waller, P.R., and Sauer, R.T. (1996). Role of a peptide tagging system in degradation of proteins synthesized from damaged messenger RNA. Science *271*, 990–993.

Kessel, M., Maurizi, M.R., Kim, B., Kocsis, E., Trus, B.L., Singh, S.K., and Steven, A.C. (1995). Homology in structural organization between *E. coli* ClpAP protease and the eukaryotic 26 S proteasome. J. Mol. Biol. *250*, 587–594.

Kraulis, P.J. (1991). MOLSCRIPT: a program to produce both detailed and schematic plots of protein structures. J. Appl. Crystallogr. *24*, 946–950.

Laney, J.D., and Hochstrasser, M. (1999). Substrate targeting in the ubiquitin system. Cell *97*, 427–430.

Lanzetta, P.A., Alvarez, L.J., Reinach, P.S., and Candia, O.A. (1979). An improved assay for nanomole amounts of inorganic phosphate. Anal. Biochem. *100*, 95–97.

Laskowski, R., MacArthur, M., Hutchinson, E., and Thorton, J. (1993). PROCHECK: a program to check the stereochemical quality of protein structures. J. Appl. Crystallogr. *26*, 283–291.

Levchenko, I., Luo, L., and Baker, T.A. (1995). Disassembly of the

Mu transposase tetramer by the ClpX chaperone. Genes Dev. *9*, 2399–2408.

Levchenko, I., Seidel, M., Sauer, R.T., and Baker, T.A. (2000). A specificity-enhancing factor for the ClpXP degradation machine. Science *289*, 2354–2356.

Merritt, E.A., and Bacon, D.J. (1997). Raster3D: photorealistic molecular graphics. In Methods in Enzymolpgy, C.W. Carter, Jr., and R.M. Sweet, eds. (New York: Academic Press), pp. 505–524.

Nevskaya, N., Tischenko, S., Fedorov, R., Al-Karadaghi, S., Liljas, A., Kraft, A., Piendl, W., Garber, M., and Nikonov, S. (2000). Archaeal ribosomal protein L1: the structure provides new insights into RNA binding of the L1 protein family. Structure *8*, 363–371.

Ortega, J., Singh, S.K., Ishikawa, T., Maurizi, M.R., and Steven, A.C. (2000). Visualization of substrate binding and translocation by the ATP-dependent protease, ClpXP. Mol. Cell *6*, 1515–1521.

Otwinowski, Z., and Minor, W. (1997). Processing of X-ray diffraction data collected in oscillation mode. In Methods in Enzymology, C.W. Carter, Jr., and R.M. Sweet, eds. (New York: Academic Press), pp. 307–326.

Retallack, D.M., and Friedman, D.I. (1995). A role for a small stable RNA in modulating the activity of DNA-binding proteins. Cell *83*, 227–235.

Roche, E.D., and Sauer, R.T. (1999). SsrA-mediated peptide tagging caused by rare codons and tRNA scarcity. EMBO J. *18*, 4579–4589.

Roche, E.D., and Sauer, R.T. (2001). Identification of endogenous SsrA-tagged proteins reveals tagging at positions corresponding to stop codons. J. Biol. Chem. *276*, 28509–28515.

Sack, J.S. (1988). CHAIN: a crystallographic modeling program. J. Mol. Graph. *6*, 244–245.

Schweder, T., Lee, K.H., Lomovskaya, O., and Matin, A. (1996). Regulation of *Escherichia coli* starvation sigma factor (sigma s) by ClpXP protease. J. Bacteriol. *178*, 470–476.

Song, H.K., Hartmann, C., Ramachandran, R., Bochtler, M., Behrendt, R., Moroder, L., and Huber, R. (2000). Mutational studies on HslU and its docking mode with HslV. Proc. Natl. Acad. Sci. USA *97*, 14103–14108.

Sousa, M.C., Trame, C.B., Tsuruta, H., Wilbanks, S.M., Reddy, V.S., and McKay, D.B. (2000). Crystal and solution structures of an HslUV protease-chaperone complex. Cell *103*, 633–643.

Terwilliger, T.C., and Berendzen, J. (1999). Automated MAD and MIR structure solution. Acta Crystallogr. D *55*, 849–861.

Vagin, A., and Teplyakov, A. (2000). An approach to multi-copy search in molecular replacement. Acta Crystallogr. D *56*, 1622–1624.

Verma, R., and Deshaies, R.J. (2000). A proteasome howdunit: the case of the missing signal. Cell *101*, 341–344.

Voges, D., Zwickl, P., and Baumeister, W. (1999). The 26S proteasome: a molecular machine designed for controlled proteolysis. Annu. Rev. Biochem. *68*, 1015–1068.

Wah, D.A., Levchenko, I., Baker, T.A., and Sauer, R.T. (2002). Characterization of a specificity factor for an AAA+ ATPase: assembly of SspB dimers with ssrA-tagged proteins and the ClpX hexamer. Chem. Biol. *9*, 1237–1245.

Wallace, A.C., Laskowski, R.A., and Thornton, J.M. (1995). LIGPLOT: a program to generate schematic diagrams of protein-ligand interactions. Protein Eng. *8*, 127–134.

Wang, J., Hartling, J.A., and Flanagan, J.M. (1997). The structure of ClpP at 2.3 Å resolution suggests a model for ATP-dependent proteolysis. Cell *91*, 447–456.

Wang, L., Elliott, M., and Elliott, T. (1999). Conditional stability of the HemA protein (glutamyl-tRNA reductase) regulates heme biosynthesis in *Salmonella typhimurium*. J. Bacteriol. *181*, 1211–1219.

Wang, J., Song, J.J., Franklin, M.C., Kamtekar, S., Im, Y.J., Rho, S.H., Seong, I.S., Lee, C.S., Chung, C.H., and Eom, S.H. (2001). Crystal structures of the HslVU peptidase-ATPase complex reveal an ATP-dependent proteolysis mechanism. Structure *9*, 177–184.

Williams, M.D., Ouyang, T.X., and Flickinger, M.C. (1994). Starvation-induced expression of SspA and SspB: the effects of a null mutation in sspA on *Escherichia coli* protein synthesis and survival during growth and prolonged starvation. Mol. Microbiol. *11*, 1029–1043.

Withey, J.H., and Friedman, D.I. (2002). The biological roles of trans-translation. Curr. Opin. Microbiol. *5*, 154–159.

Wojtkowiak, D., Georgopoulos, C., and Zylicz, M. (1993). Isolation and characterization of ClpX, a new ATP-dependent specificity component of the Clp protease of *Escherichia coli*. J. Biol. Chem. *268*, 22609–22617.

Zeth, K., Ravelli, R.B., Paal, K., Cusack, S., Bukau, B., and Dougan, D.A. (2002). Structural analysis of the adaptor protein ClpS in complex with the N-terminal domain of ClpA. Nat. Struct. Biol. *9*, 906–911.

Accession Numbers

Atomic coordinates of the SspB127 and full-length SspB complexed with SsrA peptide have been deposited in the Protein Data Bank under ID codes 1OX8 and 1OX9, respectively.